JOINT EUROPEAN TORUS

JET–P(90)72

P.E. Stott
and JET Team

Present Status and Future Developments of JET Diagnostics

Present Status and Future Developments of JET Diagnostics

P.E. Stott
and JET Team*

JET-Joint Undertaking, Culham Science Centre, OX14 3DB, Abingdon, UK

** See Appendix 1*

Preprint of Paper to be submitted for publication in the proceedings of the
Fifth National Meeting on High Temperature Diagnostics, Minsk, USSR., 18-22 June 1990

Present Status and Future Developments of JET Diagnostics.

P E Stott

JET Joint Undertaking, Abingdon, Oxfordshire, England

ABSTRACT

JET has an extensive range of plasma diagnostics systems that have been designed and constructed to be compatible with the requirements of a large fusion experiment that routinely produces plasmas with parameters in the range required for a fusion reactor. Many of these diagnostics are designed to continue working when tritium is used at a later phase of the JET programme. Two groups of diagnostics, for profiles and for MHD fluctuations, are reviewed in more detail and some typical results are shown. New diagnostics are being designed for the pumped divertor that will be installed as a major modification of JET as part of the proposed programme extension in the years 1992 to 1996.

INTRODUCTION

JET is the world's largest and most powerful fusion experiment and came into operation in 1983. JET's main objective is to obtain and to study plasmas with parameters and dimensions in the ranges required for a fusion reactor. The plasma cross-section is D-shaped with a major radius of 3m and vertical and horizontal minor radii up to 1.75m and 1.25m respectively. JET is operated in either limiter (up to 7MA) or open divertor (up to 5MA) configurations [1] with toroidal fields up to 3.4T. Extensive areas of the inconel walls, including the inner wall and the divertor strike points, are covered with carbon tiles. Since 1989 beryllium [2,3] has been used for the main limiters and is routinely evaporated onto the walls and carbon surfaces as a getter. Discharges are presently operated in hydrogen and deuterium but tritium will be used at a later stage. JET is heated with a mixture of

neutral beams (21MW has been achieved with 80keV deuterium beams) and ion cyclotron resonance heating (about 18MW has been achieved into the plasma for 2s duration). With both heating methods combined, a total power of 35MW has resulted in a stored plasma energy in excess of 10MJ. Planned enhancements to the heating systems will raise the total power to over 40MW. A prototype lower hybrid current drive system (3.7GHz) will start to operate during 1990.

JET has approximately 50 diagnostic systems. Their status at the end of 1989 is summarized in Table I. The design of most of these started in 1979 and many European fusion laboratories have been involved in their construction and operation. The first systems were ready for the start-up of JET in 1983 and most of the others were operating by 1986. Since then most diagnostics have been developed further, many have been extensively modified for various reasons, a few are no longer used and a few new systems have been added. It is clearly impractical to attempt to review all 50 systems and so this paper will concentrate on a few typical diagnostics.

This relatively large number of diagnostic systems is needed in order to measure the many parameters that are needed to characterize a hot fusion plasma and to cover JET's wide range of different operating conditions. It is interesting to note that while JET was being constructed, many people doubted the need for anything more than the very basic diagnostics, but once JET began to operate, it was recognised that even with so many systems there are many plasma quantities that remain poorly determined. Whenever possible the most important parameters in JET are measured by at least two independent methods in order to ensure reliability. Experience has show that careful comparisons between different measurement methods (Thomson scattering and ECE) can be used to reduce the systematic errors in the separate measurements and in some cases to deduce additional data [4].

The dimensions of the JET experiment are very large with a total plasma volume of about 100 m^3. Many lines of sight are required to measure plasma profiles with a good spatial resolution (typically a few cm) and to cover the various poloidal configurations that are used in JET. Likewise the combination of good time resolution with long discharge duration (typically 20s) produces a lot of data. Signals are digitized in CAMAC modules and later stored and analyzed in a network of NORD and IBM computers.

Approximately 15 megabytes of diagnostic data are stored for each discharge and, after validation by the diagnostic physicists, can be accessed for further analysis by all JET staff.

DIAGNOSTIC ENGINEERING

JET's large physical dimensions (the mid plane of the plasma is 6m above the floor level) have required substantial engineering structures for many diagnostic systems. All diagnostic systems, particularly those with vacuum connections to the tokamak, have to be compatible with the very high standards of engineering specified for all JET component systems. These requirements, combined with the need for tritium compatibility and remote handling, have made it necessary to engineer the JET diagnostic systems to a much greater extent than was the norm for diagnostics on previous generations of fusion experiments.

Tritium will be used during JET's final phase (on the basis of present planning this will start in 1995). The main JET machine systems and many diagnostic systems have been specified to be compatible with a total yield of 10^{24} neutrons over a two year period. Good diagnostics will continue to be required during this phase. About 75% of the present systems have been radiation hardened and engineered for remote handling in order to be able to remove and, when appropriate, replace them under active conditions when personnel access will not be possible. Radiation hardening has usually been achieved by avoiding sensitive components or by locating them outside the biological shielding wall although this approach inevitably results in transmitting signals over distances up to 100m. A few systems located closer to the torus have localized radiation shields to reduce the background radiation. Some diagnostics (VUV spectroscopy, X-ray diodes, charge-exchange neutral particles, infra red cameras etc.) could not be sufficiently well shielded or located outside the torus hall but are required for the earlier phases of JET's programme. These systems will be removed for the tritium phase.

Many of the JET diagnostics were built under contract by other fusion laboratories. Stringent interface standards were imposed by JET to maintain compatibility with other machine systems and to ensure consistency between

the individual elements of the complete set of diagnostics. A similar procedure will be required for ITER. The experience gained at JET shows that is is essential to plan the diagnostics for a major fusion experiment as an integrated measurement system. This can be achieved only if the detailed work carried out in separate institutes is coordinated by a strong and experienced central team. The total cost of the JET diagnostics systems is about 10^8 US$. The effort for the design, manufacture, installation, commissioning and operation of the complete set of JET diagnostics now totals about 1000 man years. These figures for diagnostics correspond to about 10% of the overall costs and effort invested into JET since 1978. This experience can be used as a rough guide to the budget and staff numbers that will be required for ITER diagnostics.

PROFILE MEASUREMENTS

Electron Density

Electron density profiles in JET are measured with multi-channel far infra-red (FIR) interferometry, microwave reflectometry and LIDAR Thomson scattering. The FIR interferometer [5] is based on a DCN laser operating at a wavelength of 195μm. This system originally had 7 vertical and 3 lateral channels but 1 vertical and 1 lateral channel have been lost due to a shortage of ports. The vertical channels operate in a single pass mode and are supported by a large frame in order to reduce the effects of vibrations. The lateral channels are double pass using reflectors mounted on the inside wall of the torus. Radial movements of the internal mirrors of up to 1cm are corrected to within 0.02mm using a compensating interferometer at a wavelength of 119μm.

The microwave reflectometer [6] uses 12 separate frequencies in the range 18 to 80 GHz corresponding (in the O mode polarization) to densities in the range 3×10^{18} to 8×10^{19} m^{-3}. The system employs a novel narrow band sweep technique to measure the density profile with an estimated uncertainty of ±5cm. Good agreement is generally found when profiles measured with the reflectometer are compared with those measured with the interferometer and with Thomson scattering (figure 1). Density profiles for the edge of an H-mode plasma confirm the existence of a very steep density gradient

($>4x10^{20}m^{-4}$) at the plasma edge. The reflectometer data indicate that the profile may be considerably steeper than can be resolved by the other techniques.

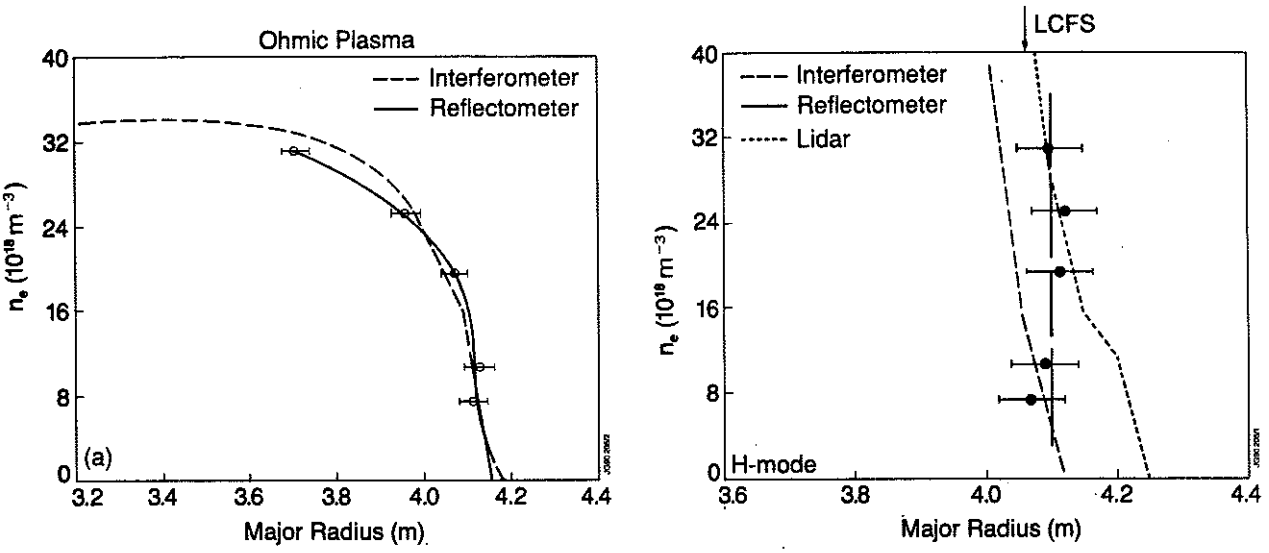

Figure 1a) Density profiles for an ohmic plasma (Ip = 4.1MA, B_T = 2.8T)

b) Section of density profiles for H-mode plasma (Ip = 3.1MA, B_T = 2.2T, P_{NB} = 8.5MW)
Peak density was 6.3 x 10^{19} m^{-3}.

Electron Temperature

Electron temperature profiles are measured with LIDAR Thomson scattering and with electron cyclotron emission (ECE). Measurements with the first JET Thomson scattering diagnostic were limited to a single spatial point on the equatorial mid-plane, although this could be scanned to different major radii between plasma shots. A 90^0 scattering geometry was used with a repetitively pulsed (1Hz) ruby laser and the detectors located on the roof of the biological shielding building.

This system has now been replaced by a spatial scan Thomson scattering diagnostic based on the LIDAR principle [7]. The plasma is illuminated with a laser whose pulse duration ($3x10^{-10}$ s) is much shorter than the transit time of the light across the plasma ($8x10^{-9}$ s) so that the time of arrival of the scattered light at the detector can be related to spatial position. The system uses a back-scattering geometry and the scattered light is

analyzed using interference filters and very fast photo multipliers. The spatial resolution, which is determined by the duration of the laser pulse and by the detector time resolution (also about 3×10^{-10} s), is inherently about 15mm but can be reduced to about 9mm by deconvolution of the scattered signal taking in account the time envelop of the laser pulse.

A typical LIDAR temperature profile is shown in figure 2. The ability of the LIDAR system to measure temperature and density profiles simultaneously and along the same chord is a considerable advantage for confinement and other studies. It is planned to replace the present ruby laser (repetition rate 0.5Hz) with an Alexandrite laser with a higher repetition rate. Higher resolution systems using a streak camera detection system are planned for the plasma edge and for the pumped divertor. The LIDAR technique requires only a single port and is therefore particularly attractive for ITER.

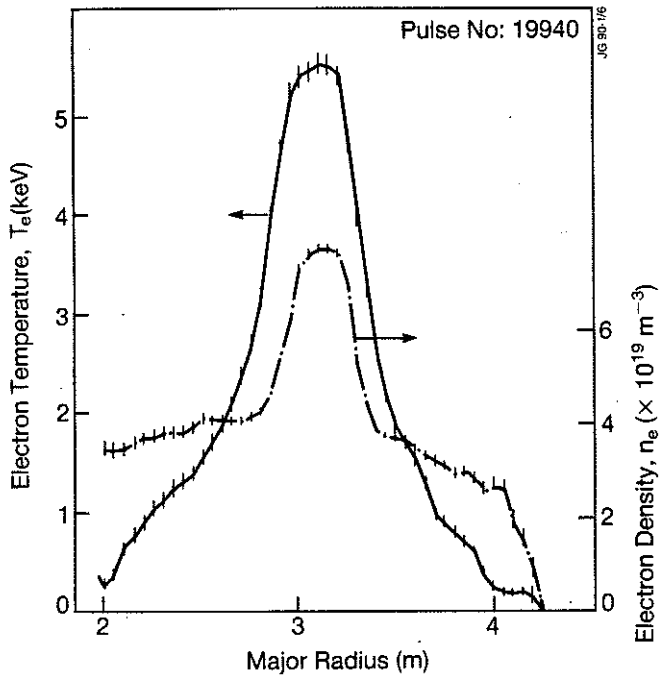

Figure 2. LIDAR electron temperature and density profiles with pellet injection and ICRH

The JET ECE system [8] has an array of 10 antennas viewing the plasma along different chords in the poloidal cross-section. The ECE emission is transmitted via oversized, rectangular metal waveguides over a distance of about 60m to the detectors which are located outside the biological

radiation shielding wall. A range of detectors optimized for different measurement purposes is used, including several Michelson interferometers (mainly used for spatial profiles with resolution of about 10cm), several Fabry-Perot interferometers, a 12 channel grating polychromator (mainly used for measurements with good time resolution and for heat pulse propagation studies of electron thermal conductivity) and a high resolution heterodyne system (spatial resolution about 2cm.). With this instrumentation ECE has been established as one of the most powerful and reliable of the JET diagnostic systems.

Ion Densities

Impurity ion densities in JET are measured with various passive spectroscopic diagnostics in the visible, VUV and XUV regions of the spectrum and with active Charge Exchange Resonance Spectroscopy (CXRS) using the heating neutral beams to illuminate the plasma. Radial profiles of the effective ion charge, Z_{eff}, are determined from Abel inverted profiles of multi-chord measurements of the visible Bremsstrahlung and from simultaneous measurements of the main light impurities by CXRS. The dilution factor n_d/n_e is determined from spectroscopic mesurements of impurity ion densities and also by combining measurements of the neutron yield (which depends on n_d and T_i) with values of T_i determined from neutron spectroscopy.

Ion Temperatures

Spectroscopic ion temperature measurements in JET are based on the Doppler broadening of spectral lines emitted either by highly ionized, high Z impurity ions (e.g. Ni^{26+}) using high resolution X-ray spectroscopy, or by fully stripped low Z impurity ions (e.g. Be^{4+} or C^{6+}) using CXRS. The Ni^{26+} resonance line emission gives the core plasma temperature and the diagnostic sensitivity permits measurements at nickel concentrations as low as $n_{Ni}/n_e = 10^{-6}$.The CXRS method is used to measure ion temperature profiles by using an array of viewing chords intersecting the neutral beam.

JET now has a single Neutral Particle Analyzer (NPA) viewing the plasma through a vertical port. This replaces the original array of 5 analyses that had to be removed at the end of 1988 from a port that was required for the Lower Hybrid Current Drive system. A new type of NPA based on a

time-of-flight technique is being developed for JET by ENEA-Frascati. This instrument will have better immunity to neutrons and γ radiation and will be usable in the tritium phase.

Several types of neutron spectrometer are operated at JET so that a wide range of plasma conditions can be covered. These include a time-of-flight system and several ^{3}He ionization chambers used for high resolution measurements ($\Delta E/E \approx 4\%$) and a liquid scintillator that is used for lower resolution studies. In many cases it is possible to unfold the neutron energy spectra to separate the thermal source from the beam plasma source and thus obtain good estimates of the central ion temperature. There is generally good agreement between the different ion temperature diagnostic methods. In ohmic discharges the ion temperature profile has been determined also from measurements of the neutron yield profile using a 19 channel collimator array.

Current Density

Polarimetric measurements of the Faraday rotation of the six vertical chords of the FIR interferometer are used to determine plasma current densities and profiles of the safety factor q. These measurements [9] indicate that in sawtoothing discharges the safety factor on the magnetic axis is always considerably less than unity and remains so even following the collapse of a monster sawtooth. Typically $q_0 = 0.75 \pm 0.15$. The change in the q profile during a sawtooth collapse has been studied by Abel inversion of the difference in the density and Faraday rotation signals before and after the collapse. The change in q during the collapse is small, typically $\Delta q_0 = 0.03$, and change in q is linear in time in between sawteeth.

An independent measurement of the q profile will be made using a modification of the single point Thomson scattering diagnostic. The strength and direction of the internal magnetic field can be determined by detecting the modulation of the scattered spectrum at angles orthogonal to the local magnetic field. This technique was demonstrated several years ago on DITE and Culham Laboratory is collaborating on the measurements on JET.

FLUCTUATIONS

JET has several diagnostics with good capability to measure the spatial distribution of plasma fluctuations. These include an X-ray diode array, and a neutron yield profile system as well as the ECE and reflectometer systems that have already been described in terms of their applications to measuring profiles. The X-ray diode system consists of about 100 detectors arranged in two orthogonal cameras in one poloidal plane with additional smaller arrays at several different toroidal locations. This diagnostic is used to investigate MHD phenomena and also to measure radiated power profiles with coarse energy resolution. Two dimensional tomography of the soft X-ray emission is used extensively to study sawteeth and disruptions. Details of a typical fast collapse of a sawtooth are shown in Figure 4. The collapse occurs on a fast time scale (about 100μs) and is not usually preceded by any precursors. A hot crescent shaped region is formed as the hot central core is displaced to one side by a cold plasma "bubble". Successor oscillations are usually seen in JET after the sawtooth collapse due to the rotation of this structure.

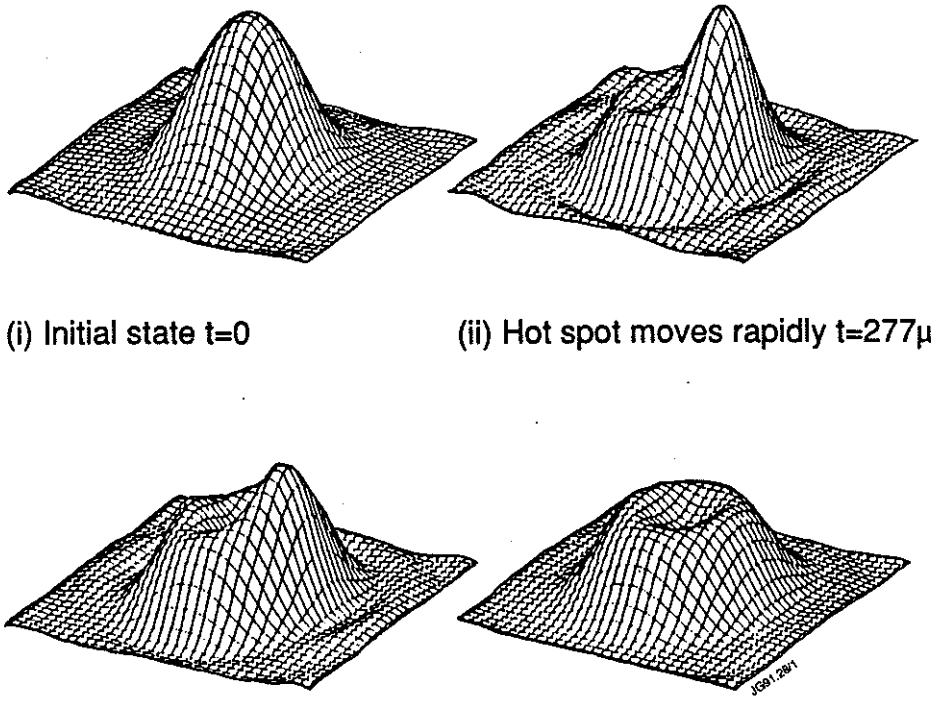

(i) Initial state t=0 (ii) Hot spot moves rapidly t=277μs

(iii) Hot spot collapses t=350μs (iv) Stable final state t=2081μs

Figure 3. Tomographic reconstructions of the X ray emissivity showing details of a sawtooth collapse.

The X-ray diagnostic has revealed an interesting effect following the injection of a solid hydrogen pellet [10]. After the initial ablation of the pellet (Figure 4), a sinusoidal perturbation appears that has, for obvious reasons, been christened "the snake". This is a local density perturbation at a rational magnetic surface, normally the q = 1 surface. It can persist for several seconds, suggesting that a magnetic island is formed at the rational surface, with ablated particles being deposited inside the island. LIDAR profiles of density and temperature after the injection of a pellet show a local density enhancement and temperature depression at the sawtooth inversion radius. This indicates local cooling at the q = 1 surface which is expected to lead to a helical current perturbation and the formation of the island.

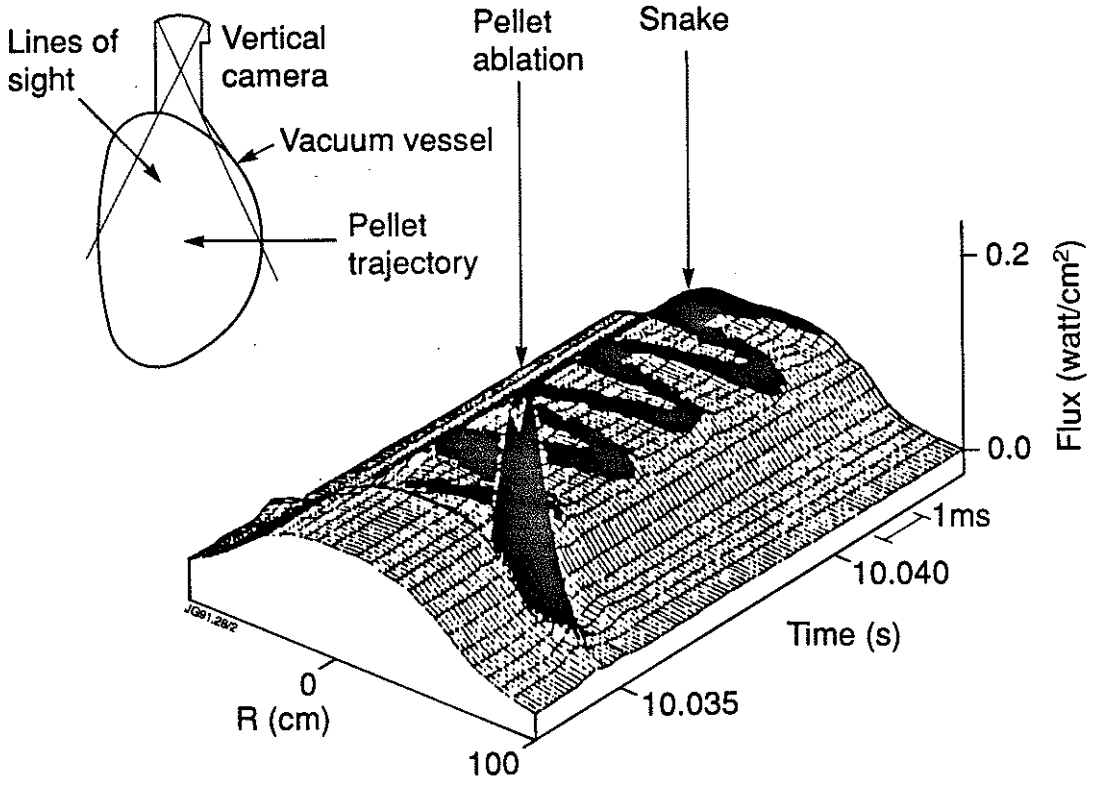

Figure 4. Details of the 'snake', a sinusoidal perturbation of the q=1 rational magnetic surface induced by pellets.

Two dimensional contours of electron temperature have been reconstructed from measurements with the 12 channel ECE polychromator. This technique utilizes the poloidal rotation of the plasma past the fixed viewing chord. Each detector sees an oscillating signal as structures in the plasma sweep past. If it is assumed that the plasma rotates as a solid body, the time variation of the signal from each detector (corresponding to a particular radius) during each period of the oscillation can be mapped as a poloidal angle. Figure 5 shows the hot core and cool island structures in the plasma following a sawtooth crash. There is good agreement between the X-ray and ECE data on island structures.

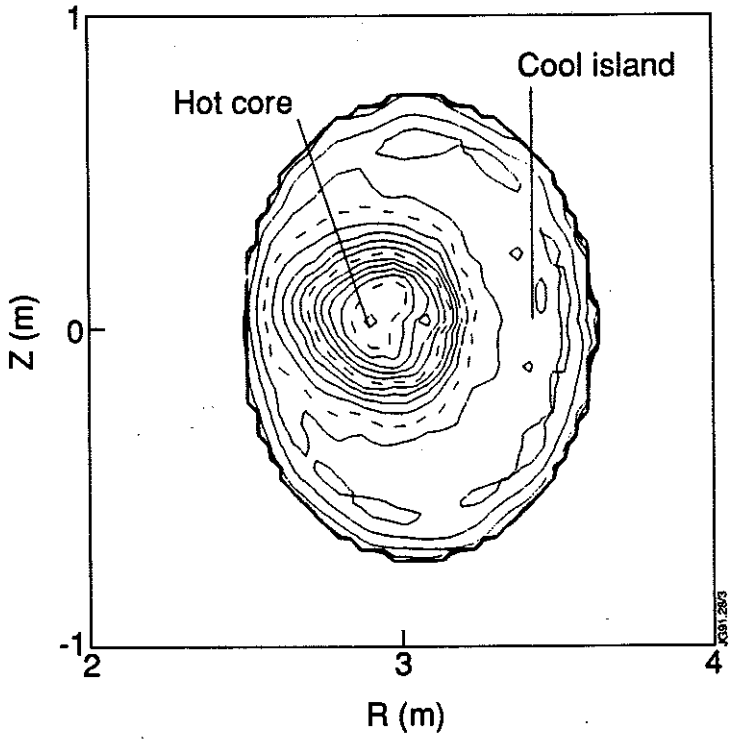

Figure 5. Hot core and cool island strutures following a sawtooth collapse shown by ECE tomography.

Neutron emission profiles are measured with a 10 channel collimator viewing horizontally and a 9 vertical channels. The detectors are low resolution neutron spectrometers (energy resolution $\Delta E/E = 8\%$) which select neutrons with energies in the range 2 to 3 MeV and discriminate against background gamma radiation. The neutron emissivity is evaluated using standard tomographic inversion methods. A sawtooth crash (figure 6) produces a dramatic change in the neutron emissivity, which before the crash is strongly centrally peaked (typical peak emissivity around 2 10^{15} m^{-3} s^{-1}) and becomes much flatter and broader afterwards.

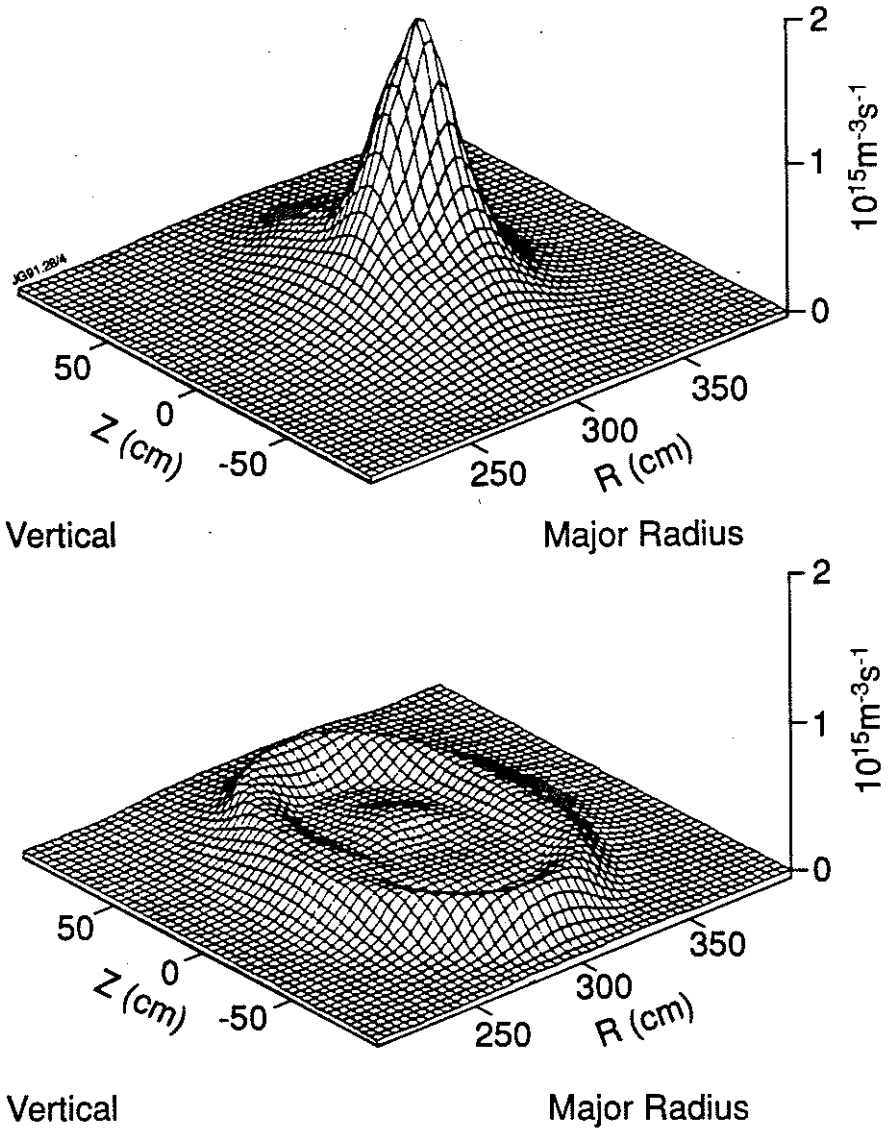

Figure 6. Tomographically inverted neutron emissivity showing the dramatic change in the emission from the core following a sawtooth crash.

FUTURE DEVELOPMENTS

Developments and upgrades are planned for many of the JET diagnostics. An upgrade is planned for the LIDAR Thomson scattering system to increase the repetition rate from 0.5Hz towards a goal of 10Hz. Following an initial survey of possible lasers, an Alexandrite laser appeared suitable for this application, but recent tests are not so encouraging and suggest that it may not be possible to achieve the required combination of repetition rate (10Hz), pulse duration (350ps) and energy (>1J). Alternative solutions including the consequences of accepting a longer pulse duration are being considered. Another upgrade of the LIDAR diagnostic using a streak camera will improve the spatial resolution (presently about 9cm) for measurements closer to the plasma edge.

In the new phase of JET that is planned for 1992 - 1996, a pumped divertor will be installed with coils and a cryopump inside the vacuum vessel. A single null configuration will be used with the X-point at the bottom of the torus. The plasma parameters in the vicinity of the X-point will be substantially different from those in the core plasma with electron densities in the range 3×10^{19} to $2 \times 10^{20} m^{-3}$ and temperatures in the range 10 to 100eV. There will be strong gradients along and perpendicular to the field lines. Access is severely restricted by the divertor coils and other components. A range of new diagnostics is being planned including; interferometry, reflectometry, electron cyclotron absorption, Thomson scattering, VUV and visible light spectroscopy, bolometry, Langmuir probes, neutral gas pressure probes, infra-red cameras and magnetic coils.

As already noted many of the JET diagnostics have been designed to operate in the tritium phase. JET has a comprehensive set of neutron diagnostics, already operational at 2.4MeV with deuterium plasmas, that will be extended for 14MeV. Some new diagnostics are planned for alpha particles and other fast ions. Charge exchange spectroscopy using the heating neutral beams (up to 80keV for H° and 160keV for D° will cover the lower range of alpha energies up to about 0.5MeV. A double charge exchange diagnostic will be built for JET by the Ioffe Institute in Leningrad. A collective scattering diagnostic based on a powerful gyrotron source (400kW at 140GHz) is planned for the higher energy alphas and will be used also for studies of energetic ions produced by various heating methods.

SUMMARY

The JET experiment has been equipped with a very comprehensive set of diagnostics. All of these systems were designed and constructed specifically for JET and were engineered to much higher standards than had previously been the norm for diagnostics. The resulting systems have proved to be very reliable in operation and routinely give high quality data. There have been many modifications and upgrades to keep pace with JET's changing requirements and with continuing developments in diagnostic techniques. JET's experience has confirmed that accurate and reliable diagnostics are essential for the safe operation and effective exploitation of a large fusion experiment. It is important that diagnostics should be regarded as an integral part of the overall machine design and in particular their requirements must be allowed to influence the design of other machine sub-systems. There is little point in building a major fusion experiment if its potential cannot be exploited because of inadequate measurement capability. The experience gained with diagnostics for JET is particularly valuable for the specification of diagnostic requirements for ITER.

ACKNOWLEDGEMENTS

It is a pleasure to acknowledge my colleagues in JET and other fusion laboratories who have contributed to this work.

REFERENCES

[1] P. J. Lomas et al. Plasma physics and Cont. Fusion, **31**, (1989) 1481.
[2] M. Keilhacker et al. JET-P(89)83.
[3] P. THomas et al. Paper presented at the 9th Plasma Surface Interactions Conference, Bournemouth, UK, May 1990. To be published in J. Nucl. Mat.
[4] A. E. Costley, Invited paper at this conference.
[5] G. Braithwaite et al. Rev. Sci. Instrum. **60** (1989) 2825.
[6] R. Prentice et al. 17th European Conference on Controlled Fusion and Plasma Heating, **IV** (1990) 1500.
[7] H. Salzmann et al. Rev. Sci. Instrum. **60** (1988) 1451.
[8] A. E. Costley, Proceedings of the Course & Workshop on Diagnostic Techniques for Fusion Plasmas, Varenna (1986) I 119.

[9] R. D. Gill et al. 16th European Conference on Controlled Fusion and Plasma Physics, Venice (1989) **II** 469.

[10] A. Weller et al. Phys. Rev. Lett., **59** (1987) 2303.

Table I
Status of the JET Diagnostics Systems, December 1989

System	Diagnostic	Purpose	Association	Status	Compatibility with tritium	Level of automation
KB1	Bolometer array	Time and space resolved total radiated power	IPP Garching	Operational	Yes	Fully automatic
KC1	Magnetic diagnostics	Plasma current, loop volts, plasma position, shape of flux surfaces, diamagnetic loop, fast MHD	JET	Operational	Yes	Fully automatic
KE1	Single point Thomson scattering	T_e and n_e at one point several times	Risø	Operational	Yes	Fully automatic
KE3	Lidar Thomson scattering	T_e and n_e profiles	JET and Stuttgart University	Operational	Yes	Fully automatic
KE5	Fast ion and alpha-particle diagnostic	Space and time resolved velocity distributions	JET	Under Development	Yes	Not yet installed
KG1	Multichannel far infrared interferometer	$\int n_e ds$ on six vertical chords and two horizontal chords	CEA Fontenay-aux-Roses	Operational	Yes	Semi-automatic
KG2	Single channel microwave interferometer	$\int n_e ds$ on one vertical chord	JET and FOM Rijnhuizen	Operational	Yes	Fully automatic
KG3	Microwave reflectometer	n_e profiles and fluctuations	JET and FOM Rijnhuizen	Operational	Yes	Fully automatic
KG4	Polarimeter	$\int n_e B_p ds$ on six vertical chords	JET and CEA Fontenay-aux-Roses	Operational	Yes	Semi-automatic
KH1	Hard X-ray monitors	Runaway electrons and disruptions	JET	Operational	Yes	Fully automatic
KH2	X-ray pulse height spectrometer	Plasma purity monitor and T_e on axis	JET	Operational	Yes	Semi-automatic
KJ1	Soft X-ray diode arrays	MHD instabilities and location of rational surfaces	IPP Garching	Operational	No	Semi-automatic
KJ2	Toroidal soft X-ray arrays	Toroidal mode numbers	JET	Operational	Yes	Semi-automatic
KK1	Electron cyclotron emission spatial scan	$T_e(r,t)$ with scan time of a few milliseconds	NPL, UKAEA Culham and JET	Operational	Yes	Fully automatic
KK2	Electron cyclotron emission fast system	$T_e(r,t)$ on microsecond time scale	FOM Rijnhuizen	Operational	Yes	Fully automatic
KK3	Electron cyclotron emission heterodyne	$T_e(r,t)$ with high spatial resolution	JET	Operational	Yes	Semi-automatic
KL1	Limiter viewing	Monitor of hot spots on limiter, walls and RF antennae, divertor target tiles	JET	Operational	No	Fully automatic
KL3	Surface temperature	Surface temperature of limiter and target tiles	JET	Commissioning	No	Will be fully automatic
KM1	2.4MeV neutron spectrometer	Neutron spectra in D-D discharges, ion temperatures and energy distributions	UKAEA Harwell	Operational	Not applicable	Semi-automatic
KM3	2.4MeV time-of-flight neutron spectrometer		NEBESD Studsvik	Operational	Not applicable	Fully automatic
KM4	2.4MeV spherical ionisation chamber		KFA Jülich	Commissioning	Yes	Semi-automatic
KM2	14MeV neutron spectrometer	Neutron spectra in D-T discharges, ion temperatures and energy distributions	UKAEA Harwell	Under Construction	Yes	Not yet installed
KM5	14MeV time-of-flight neutron spectrometer		SERC, Gothenberg		Yes	Not yet installed
KM7	Time-resolved neutron yield monitor	Triton burning studies	JET and UKAEA Harwell	Operational	Not applicable	Fully automatic
KN1	Time-resolved neutron yield monitor	Time resolved neutron flux	UKAEA Harwell	Operational	Yes	Fully automatic
KN2	Neutron activation	Absolute fluxes of neutrons	UKAEA Harwell	Operational	Yes	Semi-automatic
KN3	Neutron yield profile measuring system	Space and time resolved profile of neutron flux	UKAEA Harwell	Operational	Yes	Fully automatic
KN4	Delayed neutron activation	Absolute fluxes of neutrons	Mol	Operational	Yes	Fully automatic
KP3	Fusion product detectors	Alpha-particles produced by D-T fusion reactions	JET	Under study	Yes	Automatic
KR1	Neutral particle analyser array	Ion distribution function, $T_i(r)$	ENEA Frascati	Operational	No	Automatic
KR2	Active phase NPA	Ion distribution function, $T_i(r)$	ENEA Frascati	Under construction	Yes	Automatic
KS1	Active phase spectroscopy	Impurity behaviour in active conditions	IPP Garching	Operational	Yes	Semi-automatic
KS2	Spatial scan X-ray crystal spectroscopy	Space and time resolved impurity density profiles	IPP Garching	Operational	No	Not yet implemented
KS3	H-alpha and visible light monitors	Ionisation rate, Z_{eff}, impurity fluxes from wall and limiter	JET	Operational	Yes	Semi-automatic
KS4	Charge exchange re-combination spectroscopy (using heating beam)	Fully ionized light impurity concentration, $T_i(r)$, rotation velocities	JET	Operational	Yes	Semi-automatic
KS5	Active Balmer α spectroscopy	T_D, n_D and Z_{eff} (r)	JET	Under Construction	Yes	Not yet implemented
KT1	VUV spectroscopy spatial scan	Time and space resolved impurity densities	CEA Fontenay-aux-Roses	Operational	No	Semi-automatic
KT2	VUV broadband spectroscopy	Impurity survey	UKAEA Culham	Operational	No	Fully automatic
KT3	Active phase CX spectroscopy	Fully ionized light impurity concentration, $T_i(r)$, rotation velocities	JET	Operational in '90	Yes	Not yet implemented
KT4	Grazing incidence + visible spectoscopy	Impurity survey	UKAEA Culham	Operational	No	Fully automatic
KX1	High resolution X-ray crystal spectroscopy	Central ion temperature, rotation and Ni concentration	ENEA Frascati	Operational	Yes	Fully automatic
KY1	Surface analysis station	Plasma wall and limiter interactions including release of hydrogen isotope recycling	IPP Garching	Operational	Yes	Automated, but not usually operated unattended
KY2	Surface probe fast transfer system		UKAEA Culham	Operational	Yes	
KY3	Plasma boundary probes	Vertical probe drives for reciprocating Langmuir and surface collecting probes	JET, UKAEA Culham and IPP Garching	Operational	Yes	
KY4	Fixed Langmuir probes (X-point and belt limiter)	Edge parameters	JET	Operational	Yes	Semi-automatic
KZ1	Pellet injector diagnostic	Particle transport, fuelling	JET and IPP Garching	Operational	No	Not automatic
KZ3	Laser injected trace elements	Particle transport, T_i, impurity behaviour	JET	Operational	Yes, after modification	Not automatic
Kγ1	Gamma-rays	Fast ion distributions	JET	Operational	Yes	Manual

P T7 (rev 17/1/90)

APPENDIX 1.

THE JET TEAM

JET Joint Undertaking, Abingdon, Oxon, OX14 3EA, U.K.

J.M.Adams[1], F.Alladio[4], H.Altmann, R.J.Anderson, G.Appruzzese, W.Bailey, B.Balet, D.V.Bartlett, L.R.Baylor[24], K.Behringer, A.C.Bell, P.Bertoldi, E.Bertolini, V.Bhatnagar, R.J.Bickerton, A.Boileau[3], T.Bonicelli, S.J.Booth, G.Bosia, M.Botman, D.Boyd[31], H.Brelen, H.Brinkschulte, M.Brusati, T.Budd, M.Bures, T.Businaro[4], H.Buttgereit, D.Cacaut, C.Caldwell-Nichols, D.J.Campbell, P.Card, J.Carwardine, G.Celentano, P.Chabert[27], C.D.Challis, A.Cheetham, J.Christiansen, C.Christodoulopoulos, P.Chuilon, R.Claesen, S.Clement[30], J.P.Coad, P.Colestock[6], S.Conroy[13], M.Cooke, S.Cooper, J.G.Cordey, W.Core, S.Corti, A.E.Costley, G.Cottrell, M.Cox[7], P.Cripwell[13], F.Crisanti[4], D.Cross, H.de Blank[16], J.de Haas[16], L.de Kock, E.Deksnis, G.B.Denne, G.Deschamps, G.Devillars, K.J.Dietz, J.Dobbing, S.E.Dorling, P.G.Doyle, D.F.Düchs, H.Duquenoy, A.Edwards, J.Ehrenberg[14], T.Elevant[12], W.Engelhardt, S.K.Erents[7], L.G.Eriksonn[5], M.Evrard[2], H.Falter, D.Flory, M.Forrest[7], C.Froger, K.Fullard, M.Gadeberg[11], A.Galetsas, R.Galvao[8], A.Gibson, R.D.Gill, A.Gondhalekar, C.Gordon, G.Gorini, C.Gormezano, N.A.Gottardi, C.Gowers, B.J.Green, F.S.Griph, M.Gryzinski[26], R.Haange, G.Hammett[6], W.Han[9], C.J.Hancock, P.J.Harbour, N.C.Hawkes[7], P.Haynes[7], T.Hellsten, J.L.Hemmerich, R.Hemsworth, R.F.Herzog, K.Hirsch[14], J.Hoekzema, W.A.Houlberg[24], J.How, M.Huart, A.Hubbard, T.P.Hughes[32], M.Hugon, M.Huguet, J.Jacquinot, O.N.Jarvis, T.C.Jernigan[24], E.Joffrin, E.M.Jones, L.P.D.F.Jones, T.T.C.Jones, J.Källne, A.Kaye, B.E.Keen, M.Keilhacker, G.J.Kelly, A.Khare[15], S.Knowlton, A.Konstantellos, M.Kovanen[21], P.Kupschus, P.Lallia, J.R.Last, L.Lauro-Taroni, M.Laux[33], K.Lawson[7], E.Lazzaro, M.Lennholm, X.Litaudon, P.Lomas, M.Lorentz-Gottardi[2], C.Lowry, G.Magyar, D.Maisonnier, M.Malacarne, V.Marchese, P.Massmann, L.McCarthy[28], G.McCracken[7], P.Mendonca, P.Meriguet, P.Micozzi[4], S.F.Mills, P.Millward, S.L.Milora[24], A.Moissonnier, P.L.Mondino, D.Moreau[17], P.Morgan, H.Morsi[14], G.Murphy, M.F.Nave, M.Newman, L.Nickesson, P.Nielsen, P.Noll, W.Obert, D.O'Brien, J.O'Rourke, M.G.Pacco-Düchs, M.Pain, S.Papastergiou, D.Pasini[20], M.Paume[27], N.Peacock[7], D.Pearson[13], F.Pegoraro, M.Pick, S.Pitcher[7], J.Plancoulaine, J-P.Poffé, F.Porcelli, R.Prentice, T.Raimondi, J.Ramette[17], J.M.Rax[27], C.Raymond, P-H.Rebut, J.Removille, F.Rimini, D.Robinson[7], A.Rolfe, R.T.Ross, L.Rossi, G.Rupprecht[14], R.Rushton, P.Rutter, H.C.Sack, G.Sadler, N.Salmon[13], H.Salzmann[14], A.Santagiustina, D.Schissel[25], P.H.Schild, M.Schmid, G.Schmidt[6], R.L.Shaw, A.Sibley, R.Simonini, J.Sips[16], P.Smeulders, J.Snipes, S.Sommers, L.Sonnerup, K.Sonnenberg, M.Stamp, P.Stangeby[19], D.Start, C.A.Steed, D.Stork, P.E.Stott, T.E.Stringer, D.Stubberfield, T.Sugie[18], D.Summers, H.Summers[20], J.Taboda-Duarte[22], J.Tagle[30], H.Tamnen, A.Tanga, A.Taroni, C.Tebaldi[23], A.Tesini, P.R.Thomas, E.Thompson, K.Thomsen[11], P.Trevalion, M.Tschudin, B.Tubbing, K.Uchino[29], E.Usselmann, H.van der Beken, M.von Hellermann, T.Wade, C.Walker, B.A.Wallander, M.Walravens, K.Walter, D.Ward, M.L.Watkins, J.Wesson, D.H.Wheeler, J.Wilks, U.Willen[12], D.Wilson, T.Winkel, C.Woodward, M.Wykes, I.D.Young, L.Zannelli, M.Zarnstorff[6], D.Zasche[14], J.W.Zwart.

PERMANENT ADDRESS

1. UKAEA, Harwell, Oxon. UK.
2. EUR-EB Association, LPP-ERM/KMS, B-1040 Brussels, Belgium.
3. Institute National des Récherches Scientifique, Quebec, Canada.
4. ENEA-CENTRO Di Frascati, I-00044 Frascati, Roma, Italy.
5. Chalmers University of Technology, Göteborg, Sweden.
6. Princeton Plasma Physics Laboratory, New Jersey, USA.
7. UKAEA Culham Laboratory, Abingdon, Oxon. UK.
8. Plasma Physics Laboratory, Space Research Institute, Sao José dos Campos, Brazil.
9. Institute of Mathematics, University of Oxford, UK.
10. CRPP/EPFL, 21 Avenue des Bains, CH-1007 Lausanne, Switzerland.
11. Risø National Laboratory, DK-4000 Roskilde, Denmark.
12. Swedish Energy Research Commission, S-10072 Stockholm, Sweden.
13. Imperial College of Science and Technology, University of London, UK.
14. Max Planck Institut für Plasmaphysik, D-8046 Garching bei München, FRG.
15. Institute for Plasma Research, Gandhinagar Bhat Gujat, India.
16. FOM Instituut voor Plasmafysica, 3430 Be Nieuwegein, The Netherlands.
17. Commissiariat à L'Energie Atomique, F-92260 Fontenay-aux-Roses, France.
18. JAERI, Tokai Research Establishment, Tokai-Mura, Naka-Gun, Japan.
19. Institute for Aerospace Studies, University of Toronto, Downsview, Ontario, Canada.
20. University of Strathclyde, Glasgow, G4 ONG, U.K.
21. Nuclear Engineering Laboratory, Lapeenranta University, Finland.
22. JNICT, Lisboa, Portugal.
23. Department of Mathematics, Univeristy of Bologna, Italy.
24. Oak Ridge National Laboratory, Oak Ridge, Tenn., USA.
25. G.A. Technologies, San Diego, California, USA.
26. Institute for Nuclear Studies, Swierk, Poland.
27. Commissiariat à l'Energie Atomique, Cadarache, France.
28. School of Physical Sciences, Flinders University of South Australia, South Australia SO42.
29. Kyushi University, Kasagu Fukuoka, Japan.
30. Centro de Investigaciones Energeticas Medioambientales y Techalogicas, Spain.
31. University of Maryland, College Park, Maryland, USA.
32. University of Essex, Colchester, UK.
33. Akademie de Wissenschaften, Berlin, DDR.

CR 88.49.1A